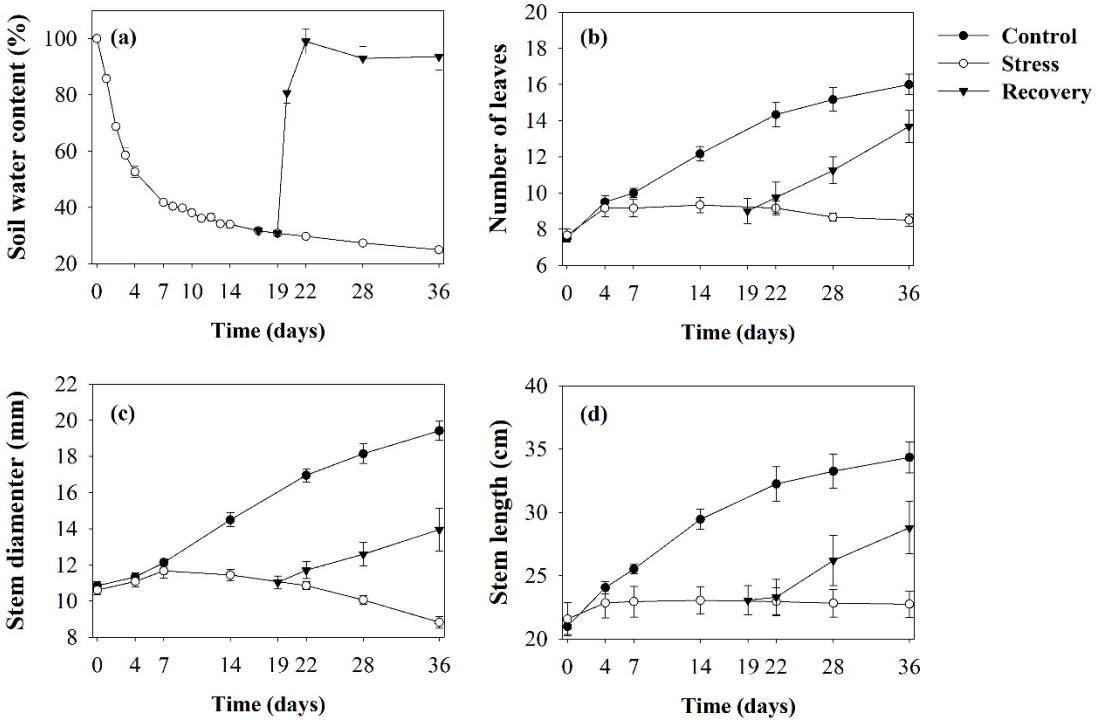

Figure S1. Effect of drought and rewatering on soil water content and plant growth. (a) soil water content, **(b)** number of leaves, **(c)** stem diameter and **(d)** stem length measured for *J. curcas* plants (46-days-old) continuously grown under well-watered conditions (Control) or subjected to drought by water withholding (Stress) followed by rewatering (Recovery). Values are means ± SE (n=4-6).

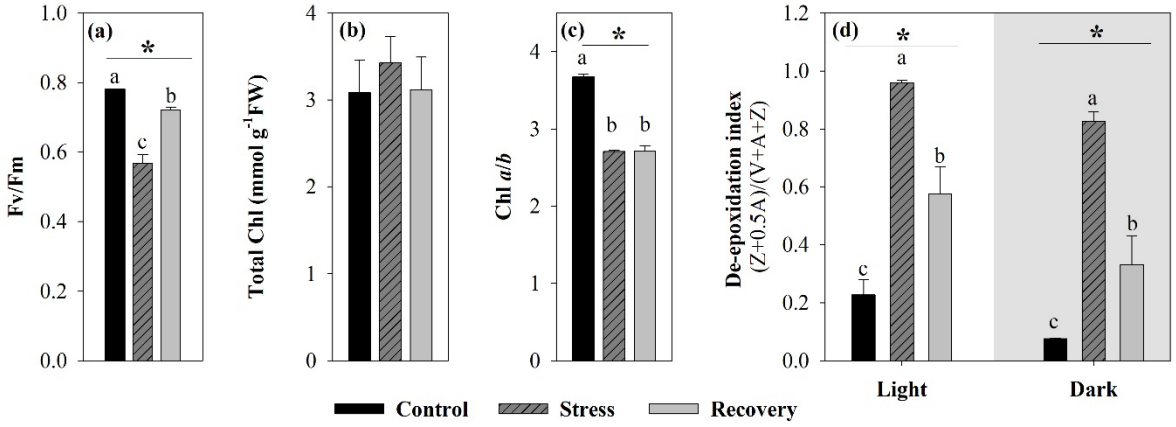

Figure S2. Effect of prolonged drought and rewatering on Chlorophyll (Chl) *a* fluorescence and leaf pigment composition. (a) Maximum quantum yield of PSII (Fv/Fm), **(b)** Total Chl content, **(c)** Chl *a* to *b* ratio and **(d)** Xanthophyll de-epoxidation index of light-adapted (3h illumination) and dark-adapted (11h darkness) leaves measured for *J. curcas* plants (46-days-old) grown under well-watered conditions (Control) or subjected to drought by water withholding (Stress) for 58 days followed by 3-days of rewatering (Recovery). Values are means ± SE (n=8 plants). V, violaxanthin; A, antheraxanthin and Z, zeaxanthin. Different letters within the same group indicate significant differences according Tukey's test (*p-value≤0.05*).

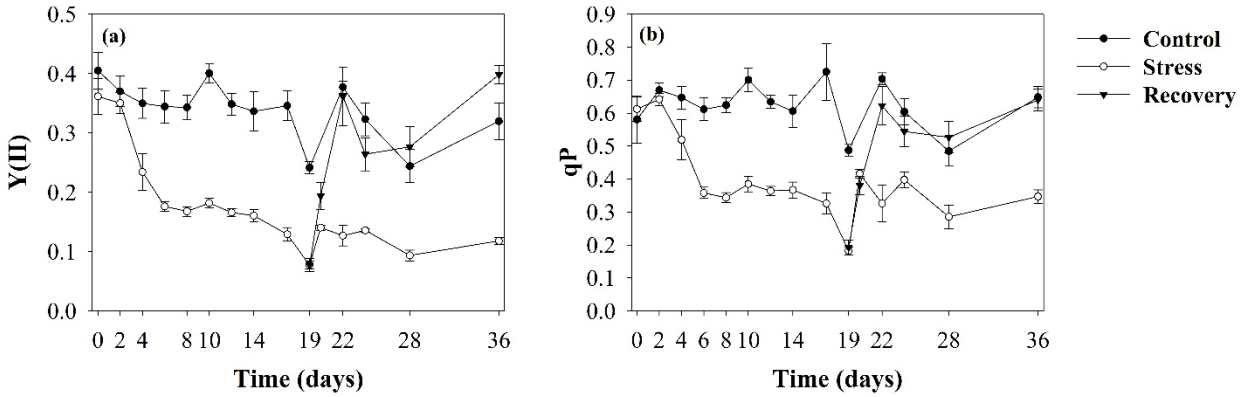

Figure S3. Effect of drought on Chl *a* fluorescence. (a) Effective photochemical quantum yield of PSII (Y(II)), **(b)** Coefficient of photochemical fluorescence quenching (qP) measured for *J. curcas* plants (46-days-old) grown under well-watered conditions (Control) or subjected to drought by water withholding (Stress) for 19 days followed by 3-days of rewatering (Recovery). Chl *a* fluorescence measurements were performed in dark-adapted leaves (≥15 min) using a leaf clip to fix the distance and the leaf area. Fo was determined with a weak measuring light followed by a saturating pulse to estimate Fm. After Fo and Fm determinations, red actinic light (440 µmol photons m^{-2} s^{-1}) was turned on, and a saturating pulse was applied every 20 s to calculate Fm' (maximum fluorescence under light), 14 pulses were performed and the last Fm' measurement was used for the calculation of Y(NPQ) and NPQ. Values are means ± SE (n=18 plants from two independent experiments, except for recovery, in which 4 plants were used).

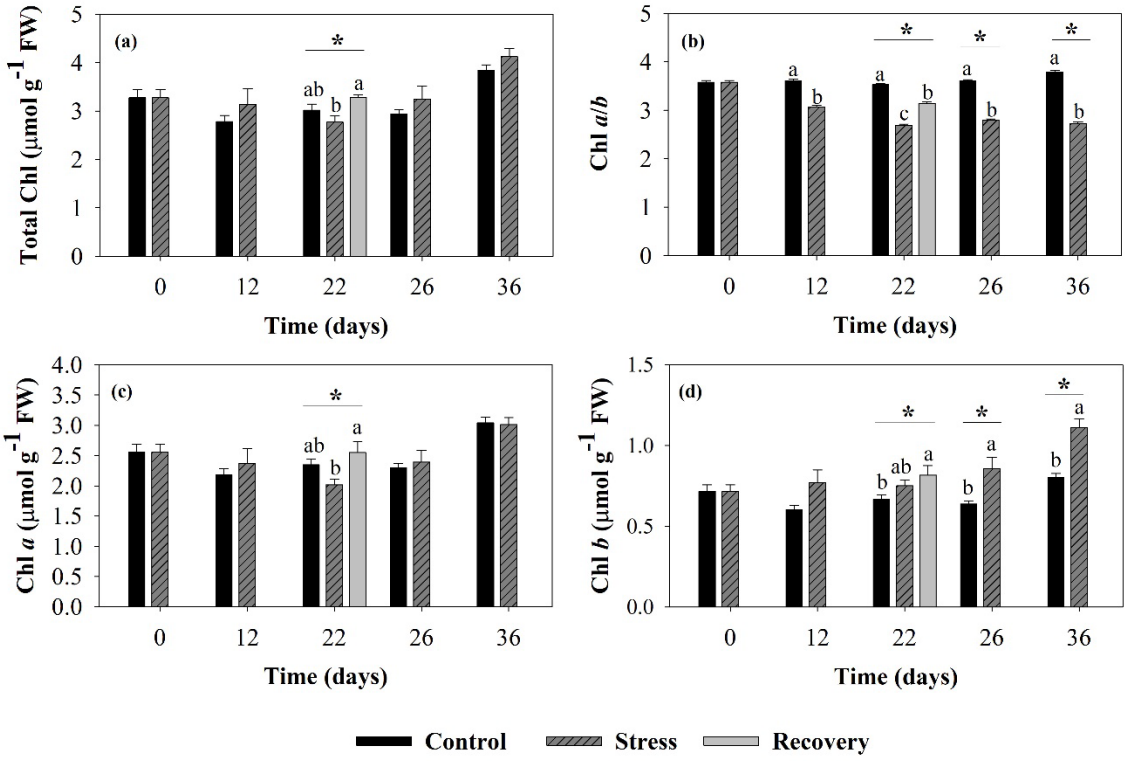

Figure S4. Effect of drought and rewatering on Chl content. (a) Total Chl, **(b)** Chl *a* to *b* ratio, **(c)** Chl *a* and **(d)** Chl *b* content of plants well-watered (Control), subjected to drought by water withholding (Stress) or 19-days of stress followed by 3-days rewatering (Recovery). Values are means ± SE (n=6 plants from two independent experiments). Different letters within the same group indicate significant differences according to t-test (*p-value≤0.05*) for pair comparisons or the Tukey's test (*p-value≤0.05*) for multiple comparisons (day 22).

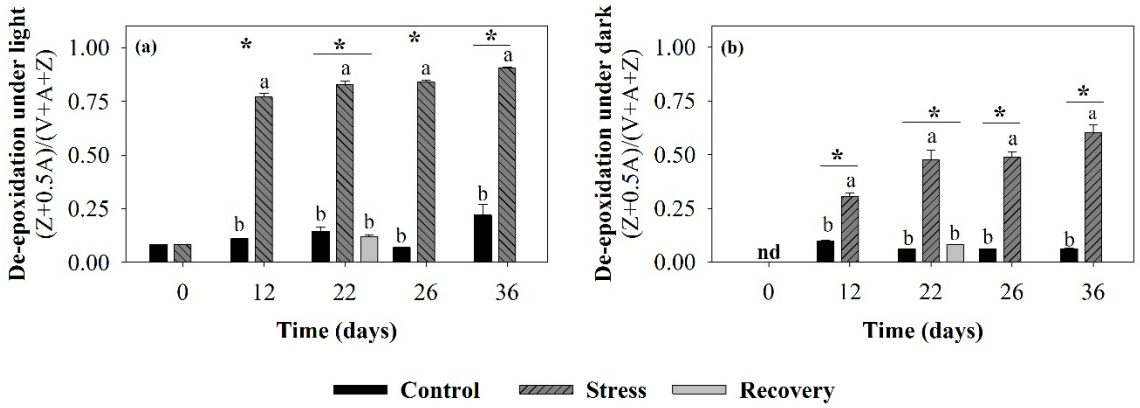

Figure S5. Effect of drought and rewatering on leaf xanthophyll de-epoxidation index. (a) Xanthophyll de-epoxidation index of light-adapted (3h illumination) and **(b)** dark-adapted (11h darkness) leaves from plants well-watered (Control), subjected to drought by water withholding (Stress) or 19-days of stress followed by 3-days rewatering (Recovery). Values are means ± SE (n=3-6 plants from two independent experiments). Nd, not determined; V, violaxanthin; A, antheraxanthin and Z, zeaxanthin. Different letters within the same group indicate significant differences according to t-test (*p-value≤0.05*) for pair comparisons or the Tukey's test (*p-value≤0.05*) for multiple comparisons (day 22).

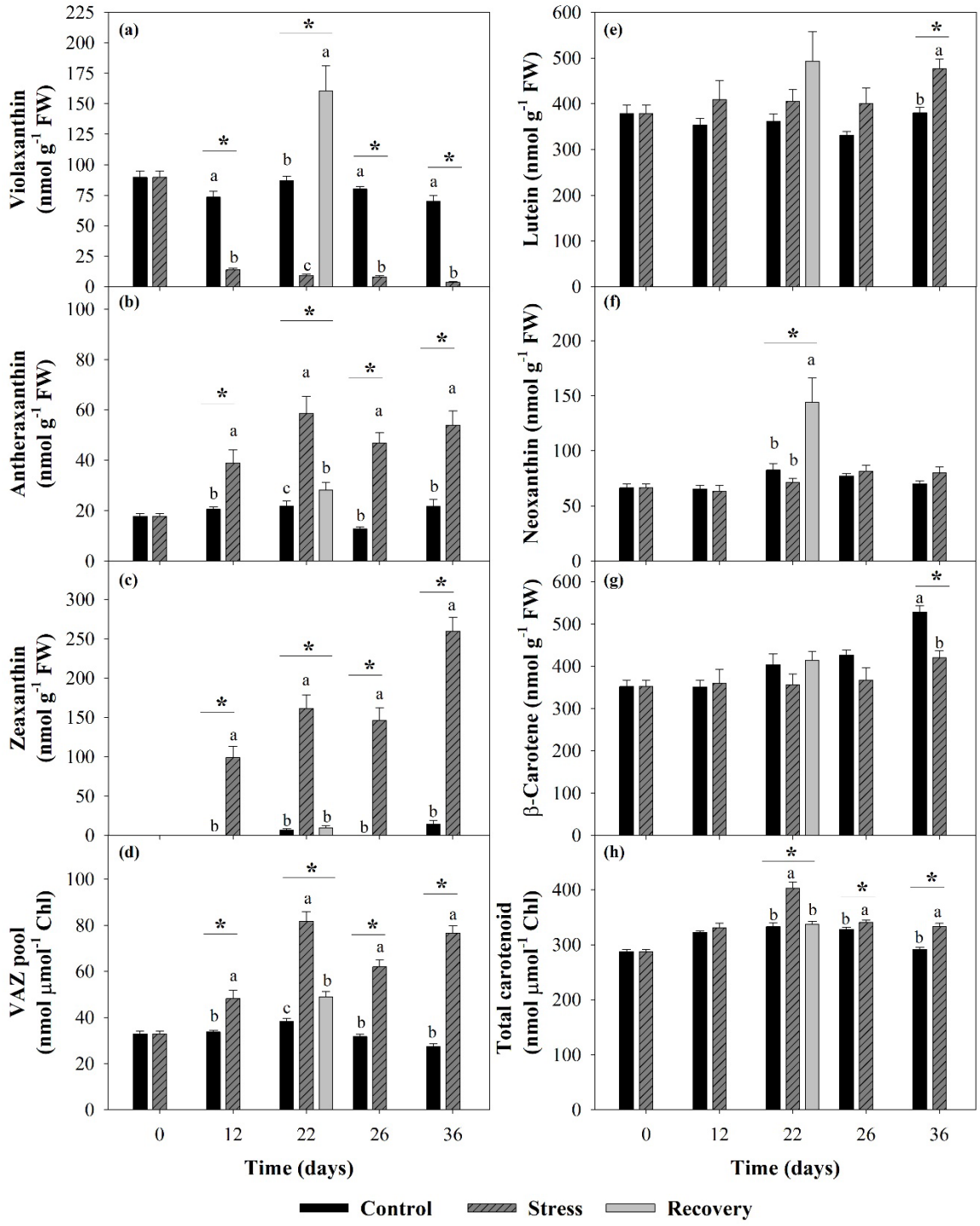

Figure S6. Effect of drought and rewatering on carotenoid content of light-adapted leaves. (a) Violaxanthin, **(b)** antheraxanthin, **(c)** zeaxanthin, **(d)** xanthophyll pool (V+A+Z), **(e)** lutein, **(f)** neoxanthin, **(g)** β-carotene and **(h)** total carotenoid content of plants well-watered (Control), subjected to drought by water withholding (Stress) or 19-days of stress followed by 3-days rewatering (Recovery). Values are means ± SE (n=6 plants from two independent experiments). Different letters within the same group indicate significant differences according to t-test (*p-value≤0.05*) for pair comparisons or the Tukey's test (*p-value≤0.05*) for multiple comparisons (day 22). V, violaxanthin; A, antheraxanthin and Z, zeaxanthin.

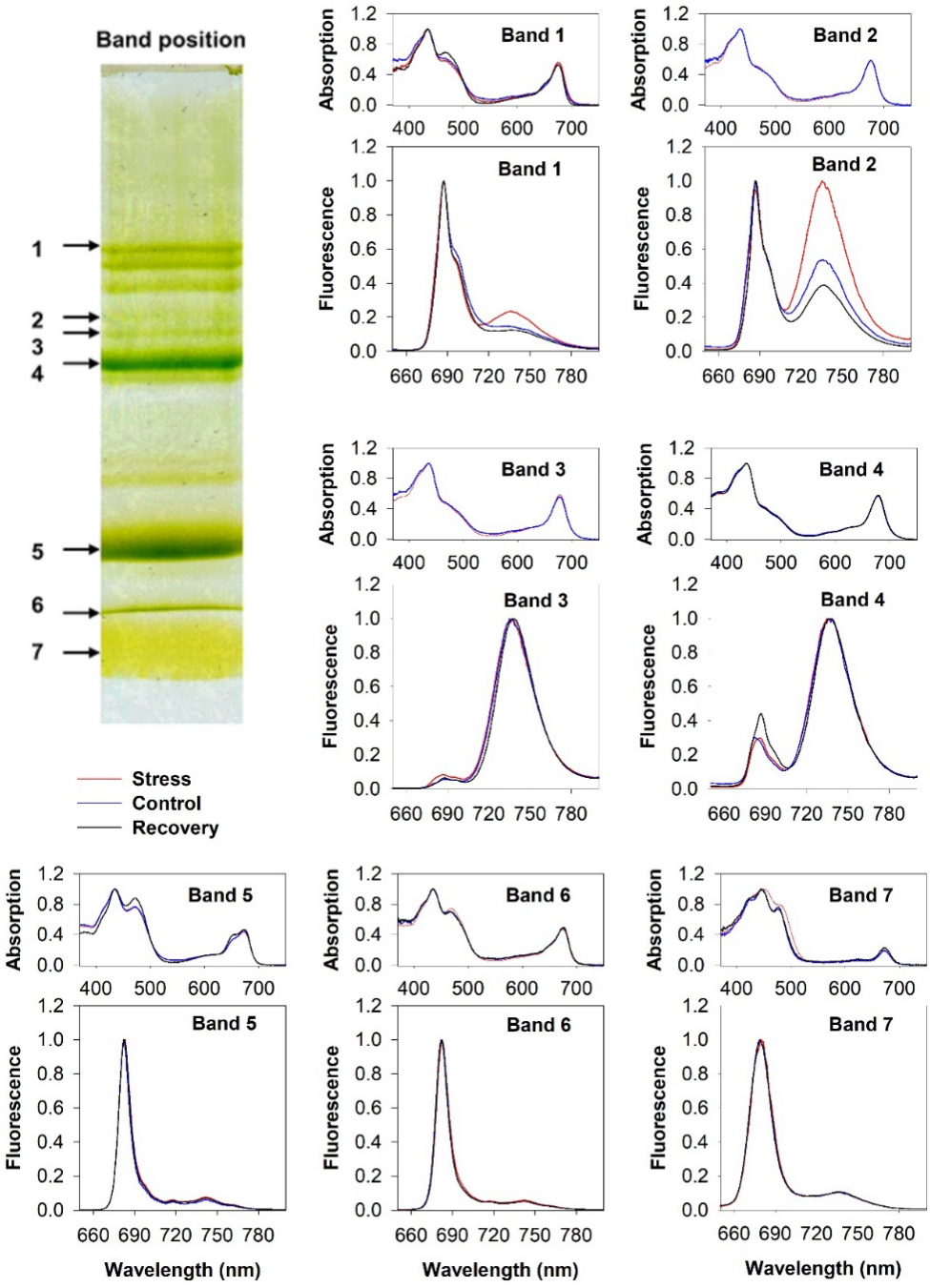

Figure S7. Steady-state relative absorption and fluorescence emission spectra of major bands isolated by lpCN-PAGE. Room temperature absorption and -196ºC fluorescence emission spectra were recorded for major bands isolated by lpCN-PAGE of 1% β-DM solubilized thylakoids isolated from control (well-watered), stress (22 days of water withholding) and recovery (19 days of water withholding + 3 days rewatering) leaves (Fig. 4a). No relative absorption for band 3 and 4 of the recovery treatment are presented due to little signal. Steady-state absorption spectra were recorded as previously described (Umetani *et al.*, 2018), using a portable photodiode array detector (EPP2000C- XR, StellarNet Inc, USA) equipped with a tungsten lamp. Steady-state fluorescence spectra were measured as described in Yokono *et al.* (2015), using an F-2500 spectrophotometer (Hitachi). The excitation wavelength was 440 nm. The optical slit widths for excitation and emission were 10 and 2.5 nm, respectively.

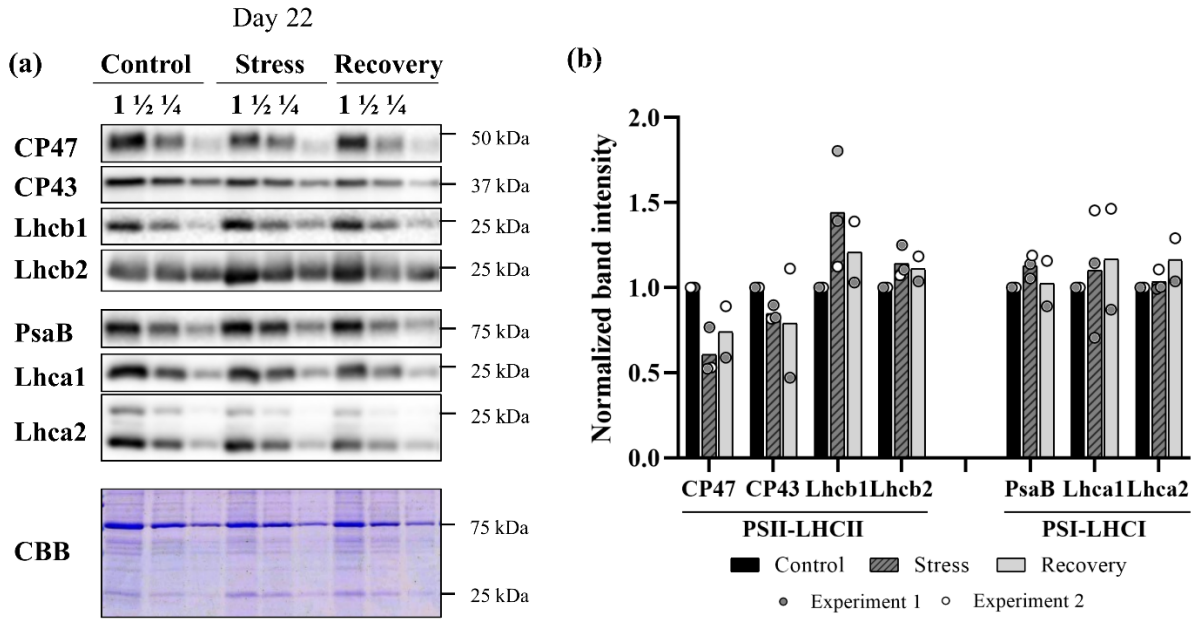

Figure S8. Drought-induced changes in the protein levels of photosystems I and II. (a) Protein samples (0.2 µg chlorophyll) extracted from leaf discs of control, stress and recovery plants at day 22 were resolved in 14 % SDS-PAGE, transferred to PVDF membranes and probed with antibodies against indicated thylakoid membrane proteins. A series of loading dilutions (1, ½, ¼) is presented for each treatment. CP43, CP47, Lhcb1 and 2 were quantified for PSII. PsaB, Lhca1 and 2 were quantified for PSI. SDS-PAGE protein gel stained with Coomassie Brilliant Blue (CBB) is presented as loading control. The molecular mass in kilodaltons (kDa) is indicated. **(b)** Quantification of chemiluminescence signals of immunoblots. Stress and recovery quantifications are shown relative to the control (set as 1.0). Bars are means and individual values are presented, tree biological samples are sown for stress and control and 2 biological samples for recovery. Biological samples were collected in two independent stress experiments. SDS-PAGE and immunoblotting was performed in duplicate.

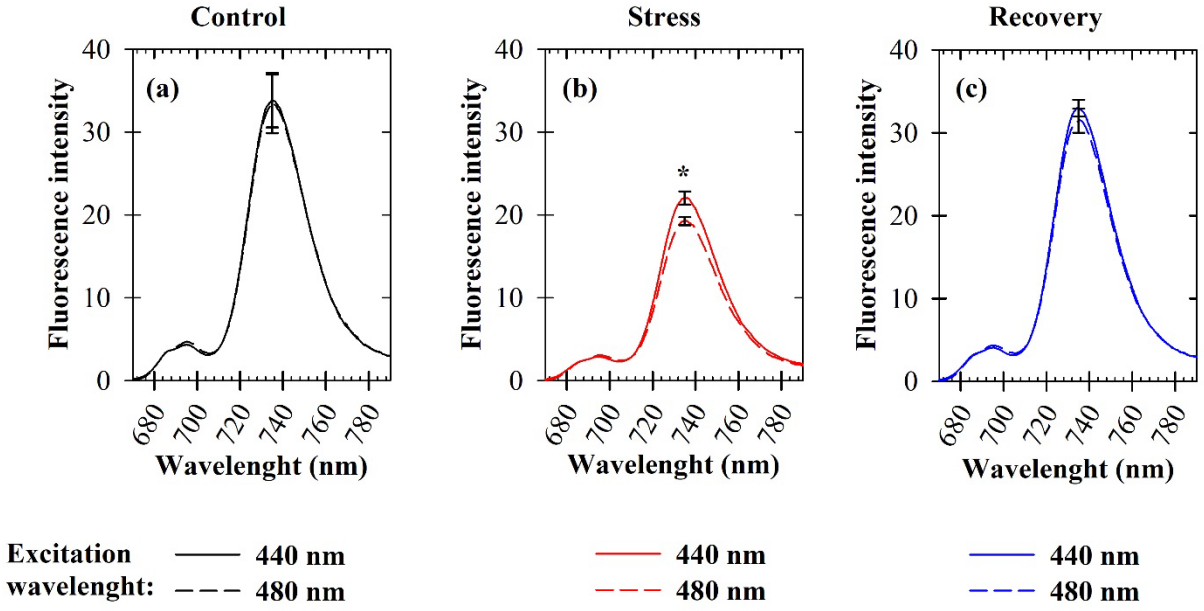

Figure S9. Effect of drought on PSII and PSI low temperature fluorescence quantum yield after excitation with 440 nm and 480 nm. Low temperature fluorescence (-196 ºC) emission spectra were measured by Integrated Sphere, samples were excited at 440 nm or 480 nm and the spectra normalized by total number of absorbed excitation photons per sample. Intact leaf discs were collected from light-adapted (3 h illumination) **(a)** control, (**b)** stress and **(c)** recovery plants. Values are means ± SE (n=3-4 plants from two independent experiments). Asterisk indicates significant differences according to t-test (*p-value≤0.05*).

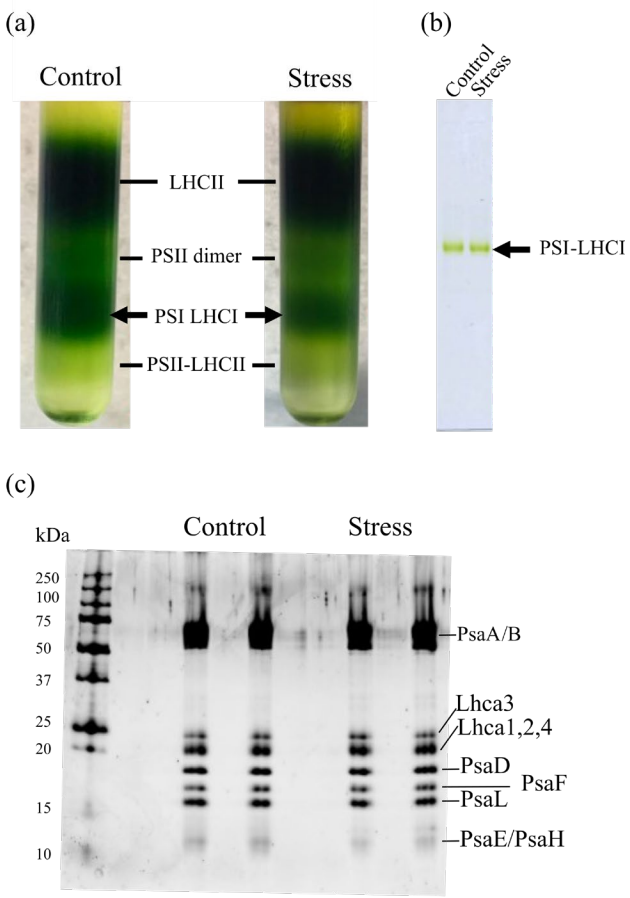

(d)

	PSI LHCI		
	Chl/Car	Chl *a*/*b*	DEI
Control	5.9	9.0	0.2
Stress	6.1	8.3	0.5

Figure S10. Purification of PSI-LHCI by sucrose-density ultracentrifugation followed by CN-PAGE. **(a)** Thylakoid membranes were isolated from control (well-watered) and stress (50-days water withholding) plants. The membranes were solubilized by 1% (w/v) β-dodecyl maltoside, and PSI-LHCI was separated by sucrose-density ultracentrifugation. The PSI-LHCI fractions indicated by arrows were collected for subsequent CN-PAGE separation. Fractions were assigned according to Dall'Osto *et al*. (2014). **(b)** CN-PAGE (gradient gel 4-14%) separation of the PSI-LHCI fraction. PSI bands were excised and subjected to the analysis of chlorophyll fluorescence using an integrating sphere (shown in Fig. 6d). **(c)** The protein in the excised PSI-LHCI band was eluted from a gel piece, subjected to SDS-PAGE and stained with silver staining. Bands were assigned according to Grebe *et al.* (2019). **(d)** Analysis of pigment compositions for the PSI-LHCI fraction from the sucrose density gradient which was subjected to CN-PAGE analysis shown in (b).

Table S1. Pigment composition of isolated photosynthetic complexes by lpCN-PAGE for plants subjected to control, stress and recovery at day 22. Pigments were normalized per 100 Chls. Values are means ± SE (n=2 leaf pool collected in independent experiments). Leaves for thylakoids isolation were collected in two independent experiments, thylakoid membrane protein solubilization and lpCN-PAGE were performed in duplicate per experiment. **PSII-LHCIIsc**, Photosystem II supercomplexes; **PSI-LHCI**, Photosystem I and light harvesting I complex; **LHCII**, light-harvesting complex II; **β-Car**, β-Carotene; Neo, Neoxanthin; **Viola**, Violaxanthin; **Anthera**, Antheraxanthin; **Zea**, Zeaxanthin; **Chl**, chlorophyll; **Car**; carotenoid; **DEI**, xanthophyll de-epoxidation index; **N.D.**, not detected.

		β-Car	Neo	Viola	Anthera	Zea	Lutein	Chl *b*	Chl *a*	Chl *a*/*b*	Total Car	DEI
PSII LHCIIsc	**Control**	6.1±1.0	2.39±0.4	2.1±0.1	0.3±0.05	0.06±0.05	10.3±0.4	22.9±0.5	77.1±0.5	3.37±0.10	21.2±1.6	0.10±0.02
	Stress	7.2±1.1	2.55±0.2	0.71±0.1	1.28±0.23	2.75±0.20	9.4±0.2	22.9±1.3	77.1±1.3	3.41±0.25	23.9±1.4	0.72±0.01
	Recovery	5.2±0.8	1.74±0.4	1.67±0.3	0.3±0.07	0.15±0.05	8.3±0.6	20.6±1.0	79.4±1.0	3.90±0.24	15.1±3.0	0.16±0.02
PSI LHCI-	**Control**	12.6±1.9	0.97±0.3	2.1±0.1	0.2±0.03	N.D.	6.0±0.2	12.4±0.5	88.6±0.9	7.19±0.28	22.3±2.5	0.05±0.01
	Stress	11.7±1.1	0.65±0.2	0.6±0.1	1.3±0.17	2.28±0.17	5.9±0.2	14.1±0.2	85.9±0.2	6.11±0.09	22.4±1.6	0.71±0.01
	Recovery	9.5±0.7	1.42±0.2	2.6±0.2	0.7±0.240	0.40±0.05	6.5±0.6	12.6±1.3	87.4±1.3	7.25±1.07	21.2±1.3	0.20±0.02
PSI LHCI	**Control**	12.2±0.4	0.22±0.12	2.2±0.09	0.3±0.01	0.02±0.02	4.6±0.1	9.5±0.1	90.5±0.1	9.56±0.13	19.5±0.7	0.07±0.01
	Stress	11.6±0.4	0.06±0.03	0.5±0.04	1.1±0.07	1.92±0.06	4.3±0.2	10.6±0.1	89.4±0.1	8.48±0.12	19.3±0.6	0.70±0.02
	Recovery	11.2±0.7	0.22±0.09	2.0±0.06	0.5±0.03	0.37±0.02	4.1±0.1	9.6±0.1	90.4±0.1	9.42±0.10	18.4±0.8	0.22±0.01
LHCII trimer	**Control**	0.1±0.02	5.7±0.2	1.6±0.05	0.2±0.04	0.03±0.03	14.9±0.7	40.5±0.3	59.5±0.3	1.47±0.02	22.6±0.6	0.08±0.02
	Stress	0.2±0.01	6.0±0.05	0.2±0.09	1.0±0.19	2.5±0.4	14.8±0.2	42.4±0.4	57.7±0.4	1.37±0.02	24.6±0.7	0.82±0.03
	Recovery	0.2±0.04	5.8±0.09	2.0±0.04	0.4±0.03	N.D.	13.5±0.4	40.8±0.2	59.2±0.2	1.45±0.02	22.0±0.5	0.10±0.01

Appendix S1 Identities of the isolated photosynthetic complexes shown in Fig. 4

The higher bands were identified as PSII-LHCII super complexes (sc) binding different amounts of LHCII (Fig. 4a). PSII-LHCIIsc bands presented the expected second dimension protein migration pattern, containing PSII-core (such as CP47/43, ~50kDa and D1/2, ~37 kDa) and Lhcb proteins (~25 kDa) (Fig. 4b) (Aro *et al.*, 2004; Järvi *et al.*, 2011). PSII-LHCIIsc also presented a typical Chl *a* enriched absorption spectrum (430 and 660 nm) and 689/697 nm low temperature fluorescence peaks (Fig. S6, band 1). In the lower PSII-LHCIIsc band, co-migration of PSI complexes was detected, as evidenced by the low temperature fluorescence 736 nm peak (Fig. S6, band 2). PSI enriched bands were displayed in the mid-section of the gel (Fig. 4a), including an upper band containing PSI-LHCI-LHCII complexes and a lower band enriched in PSI-LHCI complexes co-migrating with PSII dimer (Fig. 4a, PSI-LHCI/PSII D) (Järvi *et al.*, 2011). PSI associated bands were characterized by low fluorescence emission at RT (Fig. 4a), high β-carotene content (Table S1) and prominent 736 nm low temperature fluorescence peak (Fig. S6, band 3 and 4). Additionally, PSI associated bands presented the expected protein migration pattern, with PsaA/B (~75 kDa), Lhca 1-4 (~20 kDa) and other small PSI subunits (>20 kDa *e.g.* PsaL) (Fig. 4b) (Aro *et al.*, 2004; Järvi *et al.*, 2011). In the lower part of the gel (Fig. 4a), bands were assigned to LHCII assembly, LHCII trimer and monomer (Aro *et al.*, 2004; Järvi *et al.*, 2011). LHCII trimer enriched bands presented typical low Chl *a*/*b* (~1.5) (Fig. 4d); high Chl *b* contribution to the band absorption spectrum (450 and 640 nm) (Fig. S6, band 5); high neoxanthin content (~6 per 100 Chls) (Table S1) and Lhcb 1 and 2 as main proteins (see Fig. 7, LHCII trimer migration pattern) (Liu *et al.*, 2004; Aro *et al.*, 2004; Järvi *et al.*, 2011). The last band corresponds to free pigments, mainly carotenoids as confirmed by the 430-500 nm enriched absorption spectrum (Fig. S6, band 7). Overall, the photosynthetic complexes fractionation (Fig. 4a) and individual protein composition patterns (Fig. 4b) were similar to what is described for *Arabidopsis thaliana* (Järvi *et al.*, 2011). The exception was an unknown ~75 kDa colourless protein present in the lower part of the lpCN-PAGE gel, visible after the second dimension in all treatments (Fig. 4b). Attempts to identify this protein by mass spectrometry have failed (data not shown).

References:

Aro E-M, Suorsa M, Rokka A, Allahverdiyeva Y, Paakkarinen V, Saleem A, Battchikova N, Rintamäki E. (2004). Dynamics of photosystem II: a proteomic approach to thylakoid protein complexes. *Journal of Experimental Botany* **56**, 347–356.

Dall'Osto L, Ünlü C, Cazzaniga S, Van Amerongen H. (2014). Disturbed excitation energy transfer in Arabidopsis thaliana mutants lacking minor antenna complexes of photosystem II. *Biochimica et Biophysica Acta - Bioenergetics* **1837**, 1981–1988.

Grebe S, Trotta A, Bajwa AA, Suorsa M, Gollan PJ, Jansson S, Tikkanen M, Aro E-M. (2019). The unique photosynthetic apparatus of Pinaceae: analysis of photosynthetic complexes in Picea abies. *Journal of Experimental Botany*.

Järvi S, Suorsa M, Paakkarinen V, Aro E-M. (2011). Optimized native gel systems for separation of thylakoid protein complexes: novel super- and mega-complexes. *The Biochemical journal* **439**, 207–14.

Liu Z, Yan H, Wang K, Kuang T, Zhang J, Gui L, An X, Chang W. (2004). Crystal structure of spinach major light-harvesting complex at 2.72 Å resolution. *Nature* **428**, 287–292.

Umetani I, Kunugi M, Yokono M, Takabayashi A, Tanaka A. (2018). Evidence of the supercomplex organization of photosystem II and light-harvesting complexes in Nannochloropsis granulata. *Photosynthesis Research* **136**, 49–61.

Yokono M, Takabayashi A, Akimoto S, Tanaka A. (2015). A megacomplex composed of both photosystem reaction centres in higher plants. *Nature Communications* **6**, 6675.